

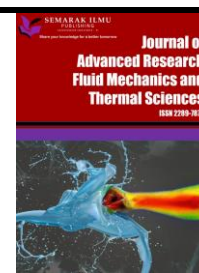


Journal of Advanced Research in Fluid Mechanics and Thermal Sciences

Journal homepage:

https://semarakilmu.com.my/journals/index.php/fluid_mechanics_thermal_sciences/index

ISSN: 2289-7879



Aqueous-phase Reforming of Glycerol using Cu-Ni Bimetal Catalyst Supported over Coconut Shell Activated Carbon

Ibrahim Yakub^{1,*}, Khairul Anwar Mohamad Said¹, Mohamed Afizal Mohamed Amin¹, Ahmad Beng Hong Kueh², Mugahed Amran^{3,4}

¹ Department of Chemical Engineering & Energy Sustainability, Faculty of Engineering, Universiti Malaysia Sarawak, 94300 Kota Samarahan, Sarawak, Malaysia

² Department of Civil Engineering, Faculty of Engineering, Universiti Malaysia Sarawak, 94300 Kota Samarahan, Sarawak, Malaysia

³ Department of Civil Engineering, College of Engineering, Prince Sattam Bin Abdulaziz University, 11942 Alkharj, Saudi Arabia

⁴ Department of Civil Engineering, Faculty of Engineering and IT, Amran University, 9677 Amran, Yemen

ARTICLE INFO

Article history:

Received 19 November 2023

Received in revised form 17 February 2024

Accepted 28 February 2024

Available online 15 March 2024

Keywords:

Glycerol; activated carbon; heterogeneous catalyst; waste-to-material

ABSTRACT

The increasing generation of glycerol as a waste from biodiesel production calls for its various consumptions, especially in producing industrial chemicals. However, the focus of popular studies in this process is on using noble metals as the catalyst. It should be shifted to a low cost and abundant element to ensure sustainability. Therefore, this study uses activated carbon from coconut shells to support a bimetal catalyst copper-nickel in converting glycerol into value-added products. The catalyst was synthesized via the wet impregnation method and was characterized using scanning electron microscopy-energy dispersive X-ray spectroscopy, Fourier-Transform infra-red spectroscopy, and a surface area analyser. It was revealed that the BET surface area (582 m²/g) is smaller than the pristine carbon because of the exposure to high temperature during calcination. The average pore size (1.7 nm) is also smaller than the coconut shell carbon due to the same effect. The surface functional groups mainly consist of carboxylic acids that is known to contribute to the hydrogenolysis of glycerol. At 20 wt% initial glycerol concentration, 20 bar and 200 °C, acetic acid, propylene oxide, carbon monoxide and acetaldehyde were detected as the products. A possible mechanism was proposed considering the aqueous-phase reforming of glycerol and the dehydration process. The optimum operating conditions in this case are 20 wt% initial glycerol concentration, 25 bar and 200 °C. More studies are needed to evaluate the reactions involved in aqueous-phase reforming of glycerol using the Cu-Ni doped on coconut shell activated carbon. In conclusion, glycerol can be converted to valuable chemicals under mild conditions by using the cost-effective catalyst.

1. Introduction

Biodiesel production is forecast to soar in 2023 due to its sustainability in replacing fossil fuels to countries such as the United States, Brazil, Malaysia and Indonesia [1,2]. Malaysia is resuming its

* Corresponding author.

E-mail address: yibrahim@unimas.my

<https://doi.org/10.37934/arfmts.115.1.193205>

biodiesel blend B20 mandate for industrial implementation that was delayed due to the pandemic in 2020, while Indonesia has announced its policy to start using B35 in 2023 [3]. A review of life-cycle analysis (LCA) of biodiesel produced from various feedstock showed that biodiesel from palm oil is the only one that meets the Renewable Energy Directive requirement with a 60% Global Warming Potential reduction concerning petroleum-based diesel [4].

Crude glycerol is generated as a by-product equivalent to 10 wt% of the biodiesel produced [5]. This could result in 6.3 million tonnes of crude glycerol by 2025 [6]. The increasing generation of glycerol is concerning since it is considered a potential pollutant especially when not treated before being released into open waters. At high concentrations, it depletes oxygen content and suffocate aquatic animals [7]. However, glycerol is a versatile intermediate in waste valorization reactions such as oxidation, pyrolysis, hydrogenolysis, etherification, esterification, dehydration, polymerization and carboxylation. The purified glycerol is also commercially consumed in the pharmaceuticals, food and beverage industries [8,9].

A desirable glycerol processing should consider the mild operating conditions (temperature and pressure), and the use of a cost-effective catalyst. Hydrogenolysis is commonly chosen to convert glycerol into propanediols in the presence of hydrogen. For that purpose, studies have shown that under mild temperature and an inert pressurized atmosphere, in-situ hydrogen via glycerol reforming could be generated as in Eq. (1) [10].



The regime of glycerol reforming can be categorized as steam reforming (SR), auto thermal reforming (ATR) or aqueous-phase reforming (APR). SR can be achieved at a high operating temperature of at least 630 °C and 1 atm (10 wt%), while the APR operating parameters are much milder to keep the water in the liquid state (e.g. 220 °C at 20 bar) [11]. In between SR and APR process conditions, it was reported that ATR occurs due to glycerol oxidation [12]. Knowledge of the reforming regime is essential in determining the possible occurring reaction.

The glycerol reforming catalyst developed to break C-O and O-H bonds was reported to be well-performed by transitional metals. The generated carbon monoxide must be consumed via a water-gas shift reaction to avoid permanent chemisorption of the catalyst surface [13]. Noble metals (i.e. Pt, Re, and Rh) are known to perform this task efficiently, but the earth-abundant elements have also been studied and proven to carry out the C-O cleavage in a glycerol reforming, including Ni, Ce, and Mg [13]. The application of Ni catalyst in the water-gas shift reaction has made it a suitable candidate for glycerol reforming due to the high CO uptake and hydrogen production [8,12,14,15]. Additionally, Cu has been shown to produce high selectivity in C-O breaking while preserving the C-C bond [16].

The catalyst support also plays an essential role in determining the catalyst's efficiency. Activated carbon has been used in glycerol hydrogenolysis due to the high density of acidic functional groups required to provide the acidic sites [17]. Gallegos-Suarez *et al.*, [18] compared glycerol consumption using carbon-supported Ru and zeolite-supported Ru and found that the former was superior by 11 - 28% conversion compared to only 7% for the zeolite-based catalyst. Nonetheless, the selectivity towards propanediol formation was lower by half because of the electron donor properties contributed by the carbon support and the precious metal that consequently generated methane. In a pursuit to replace precious metals in glycerol consumption, it is beneficial to investigate the effects of utilizing a combination of earth-abundant metals and carbon-based support. To add to the sustainability factor, biomass waste such as coconut shell, could be valorized into a catalyst support. Therefore, this work aims to investigate the possible value-added products from glycerol conversion using the developed catalyst from earth-abundant elements (Cu and Ni) and biomass-based support

(coconut shell activated carbon), under mild operating conditions. Both liquid and gaseous products of the reaction are analyzed to understand the behavior of the catalyst in the reaction.

2. Methodology

2.1 Materials

Palm kernel shell (PKS) and coconut shell (CS) activated carbons were obtained from a Malaysian supplier having particle sizes larger than 250 μm . Commercial activated charcoal Norit® (AC) was obtained from Sigma-Aldrich, UK, with 150 μm particle size measured using a particle sizer Mastersizer Aero S (Malvern Instruments, UK). PKS and CS were grounded and sieved to obtain similar size with AC.

2.2 Catalyst Synthesis

The following steps were taken to synthesize the catalyst via the wet impregnation method: Two grams of the pristine carbon (PKS and CS) were removed of moisture in a conventional oven at 110 °C for 24 hours. Then, the dried carbons were soaked in a 17-mL solution containing copper sulfate and nickel chloride at 3:1 mole ratio of Cu:Ni (deionized water as the solvent). The mixture was continuously agitated at 25 °C overnight. After that, it was dried using the oven for 24 h. The catalyst was rinsed with deionized water several times so the effluent reached pH 7. Finally, the catalyst was calcined in a furnace with static air. The furnace was heated at 20 K/min until it reached 300 °C, and held for 180 mins.

2.3 Catalyst Characterization

The surface morphology and intensity of metallic species on the catalyst were observed using a scanning electron microscopy-energy dispersive X-ray spectroscopy SEM-EDX JSM-6010LA (Jeol, USA). Before the analysis, the catalyst was coated with gold for 15 s. Then, it was positioned on the sample seat for the analysis under the electron microscope. The surface functional groups were determined qualitatively using a Fourier-Transform infra-red spectroscopy IRAffinity-1S (Shimadzu, UK) between wavenumbers from 4000 to 400 cm^{-1} . The surface area and pore properties were analyzed via a nitrogen adsorption–desorption experiment using a 3Flex Surface Analyzer (Micromeritics, USA) at 77 K.

2.4 Catalyst Activity Testing

Figure 1 shows a 45-mL batch reactor (Parr Instrument, USA) diagram used in this study to perform the glycerol conversion under a controlled environment. Five mL of glycerol solution (>99.5%) with an initial concentration of 1, 5, 20 or 30 wt%, was decanted into the reactor. After that, 0.2 g of the catalyst was added into the solution inside the reactor. The system was purged with helium gas through the inlet (V-1) and outlet (V-2), at least thrice before the pressure of the system was brought to the desired value with helium gas (20, 25 or 30 bar). Then, the temperature of the reactor was increased to 180, 190 or 200 °C at a rate of 4 K/min. The agitation was started at 1,200 rpm once the desired temperature was reached. Unless otherwise mentioned, the experiment was carried out for three hours. At the end of the reaction, the catalyst was filtered and rinsed using 5 mL acetone that was then re-mixed with the liquid-phase products to ensure minimal product losses. Note that this is a 1:1 dilution.

A sample from this dilution was further diluted for analysis as follows: 0.2 mL of the liquid sample was extracted from the product liquid-phase and equilibrated to 1.0 mL with acetone. Then, a gas chromatography-mass spectrometry (GCMS) QP2010SE (Shimadzu, UK) was used to analyze the sample. The column used was a 30-m HP-INNOWAX capillary column with 0.25 mm internal diameter and 0.25 μm film thickness (Agilent, USA). The initial GC oven was pre-heated to 45 $^{\circ}\text{C}$ where the sample was dried for 3 mins before being increased to 240 $^{\circ}\text{C}$ at a temperature ramping rate of 10 K/min. For a complete analysis, the final temperature was held for 2 mins. The injection and interface temperatures were 250 and 245 $^{\circ}\text{C}$, correspondingly. The helium flow rate was kept constant at 30 cm/s with a split ratio of 100. Moreover, the gas-phase products obtained via V-1 were collected with a gas bag. The sample was analyzed using a mass spectrometry MS Hiden HPR-20 (Hiden, UK). The MS peaks deconvolution was examined using NIST MS Search 2.0 software on fragmentation peaks.

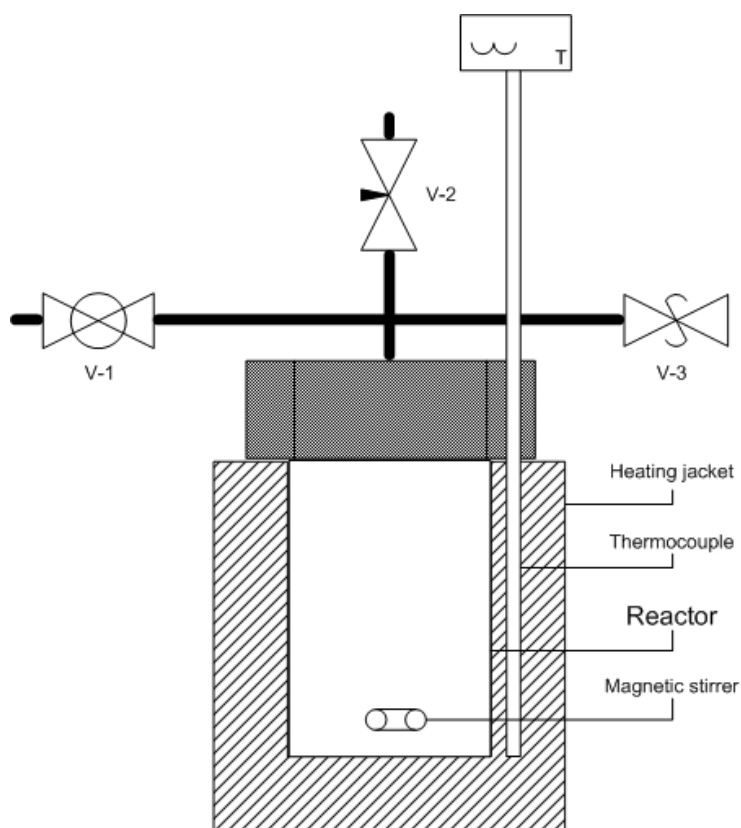


Fig. 1. Batch reactor diagram used for glycerol hydrogenolysis

3. Results

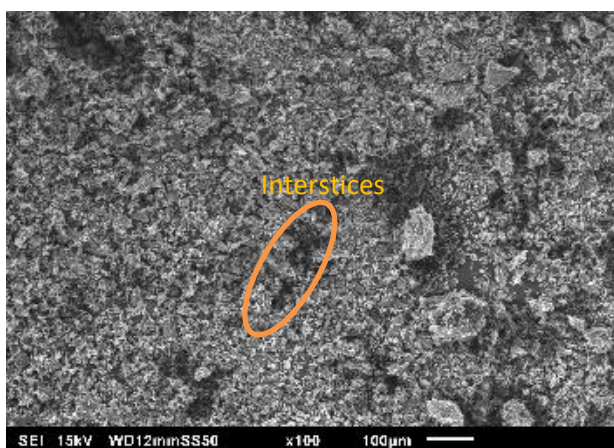
3.1 Catalyst Characteristics

The surface area, pore size and pore volume of the three carbon supports; commercial activated carbon (AC), activated carbon derived from palm kernel shell (PKS), and activated carbon derived from coconut shell (CS), are shown in Table 1. AC has the largest surface area, average pore size and pore volume. As Cu-Ni was impregnated over AC, the surface area increased while the pore volume and size decreased. The SEM images in Figure 2(a) and Figure 2(b) show that the external structure collapsed causing more interstices on CuNi/AC with most of the pores being blocked. Such a phenomenon commonly takes place over a combustible granular carbon where high temperature causes the structure to collapse [19]. On the contrary, surface area, pore size and pore volume are

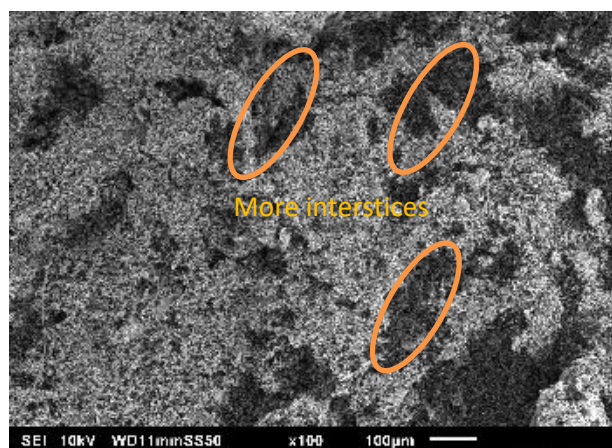
all decreased for PKS and CS upon impregnation with Cu-Ni. The SEM images in Figure 2(d) and Figure 2(f) exhibited a different structure than the pristine carbons (Figure 2(c) and Figure 2(e), correspondingly). The resultant surfaces are flattened with additional cleavages and external perforations. It can be inferred that different carbon precursors react differently during impregnation and calcination.

Table 1
 Surface properties of the catalysts

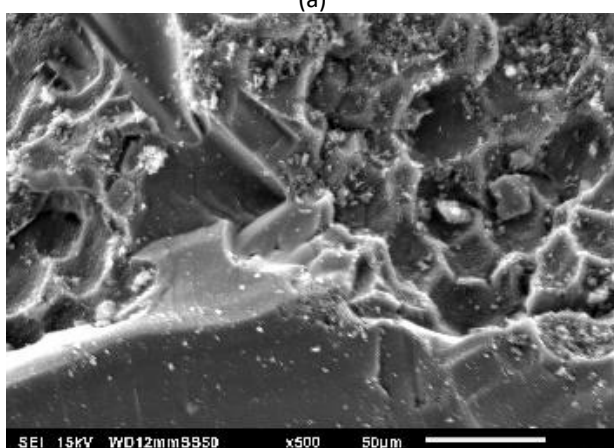
Sample	BET surface area, m ² /g	Total pore volume, cm ³ /g	Average pore size, nm
AC	1376	1.105	3.2
PKS	1126	0.526	1.8
CS	819	0.612	2.1
CuNi/AC	1739	0.486	1.1
CuNi/PKS	1013	0.430	1.7
CuNi/CS	582	0.242	1.7



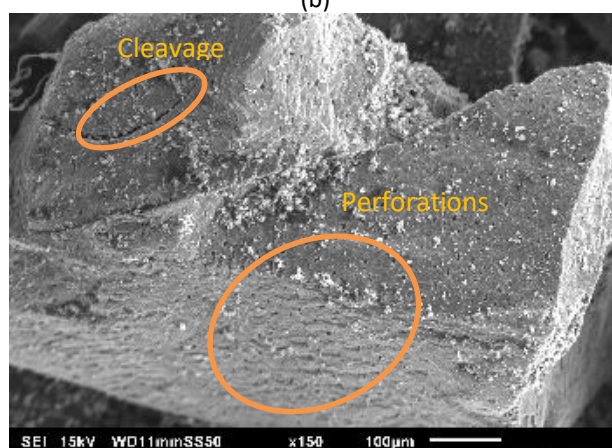
(a)



(b)



(c)



(d)

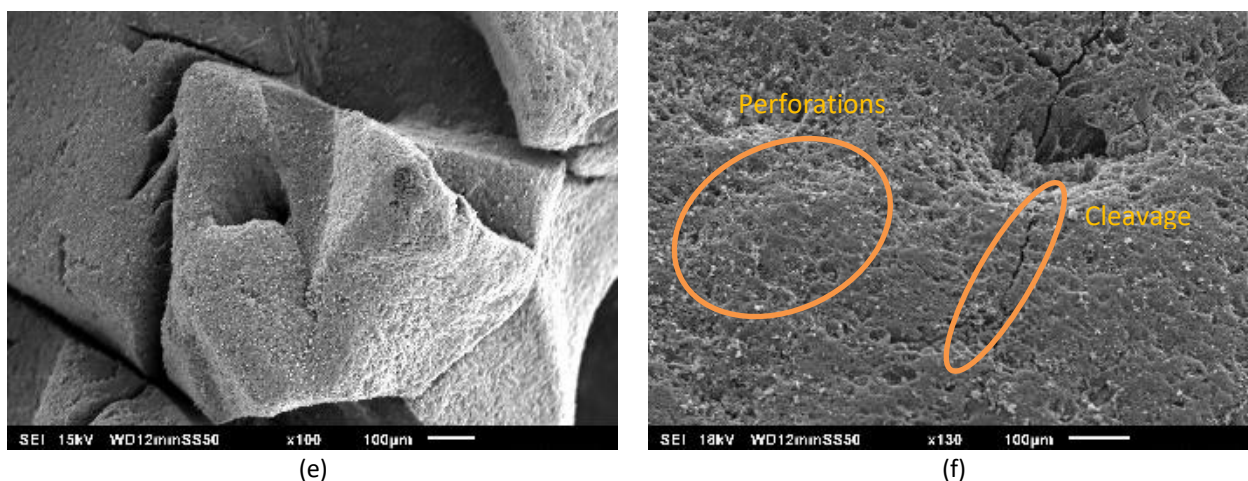


Fig. 2. SEM images for; a) AC, b) CuNi/AC, c) PKS, d) CuNi/PKS, e) CS and f) CuNi/CS

Table 2 shows the elemental analysis for inorganic elements of all samples. The impregnation of the bimetal Cu-Ni with a loading ratio of 3:1 resulted to only 2:1 ratio for CuNi/PKS and CuNi/CS while 1:1 for CuNi/AC showing the limited sites available for the catalysts especially Ni over the carbon supports. This is attributable to the higher affinity of the carbon supports towards copper than nickel [20]. In addition, the lower loadings observed over all carbon supports (as compared to the intended loadings) could also be caused by the loss of metal precursors during the process of incipient wetness.

Table 2

Inorganic elemental analysis of the catalysts

Element	AC	PKS	CS	CuNi/AC	CuNi/PKS	CuNi/CS
Si	28.6	Nd	1.2	13.2	11.3	Nd
Cl	1.6	15.4	0.3	26.6	27.9	22.6
K	Nd	35.7	8.5	Nd	0.8	0.6
Ca	2.4	3.1	0.5	1.3	Nd	0.2
Ni	Nd	Nd	0.6	18.4	12.7	19.6
Cu	Nd	Nd	0.8	13.8	25.8	46.8

*Nd = not detectable

Figure 3(a) shows the surface functional groups observed over all carbon surfaces, while Figure 3(b) shows the resulting surface functional groups over the catalysts derived from the carbon supports. It can be seen that carboxylic acids (peaks around 2600 cm^{-1} and broad peaks stretched from 1950 to 1600 cm^{-1} , denoted as β) and alkynes (various peaks within $2380 - 2000\text{ cm}^{-1}$, denoted as γ) are present over all samples but the intensity reduced after impregnation of catalyst and calcination process [21]. Carboxylic acids tend to donate protons making them a good Brønsted-Lowry acid that is preferred in the hydrogenolysis of glycerol [22]. Yu *et al.*, [23] reported that the KBH_4 treatment of a coconut shell used to support Ni greatly increased the presence of acidic groups, contributing 43% glycerol conversion and 76% 1,2-propanediol selectivity.

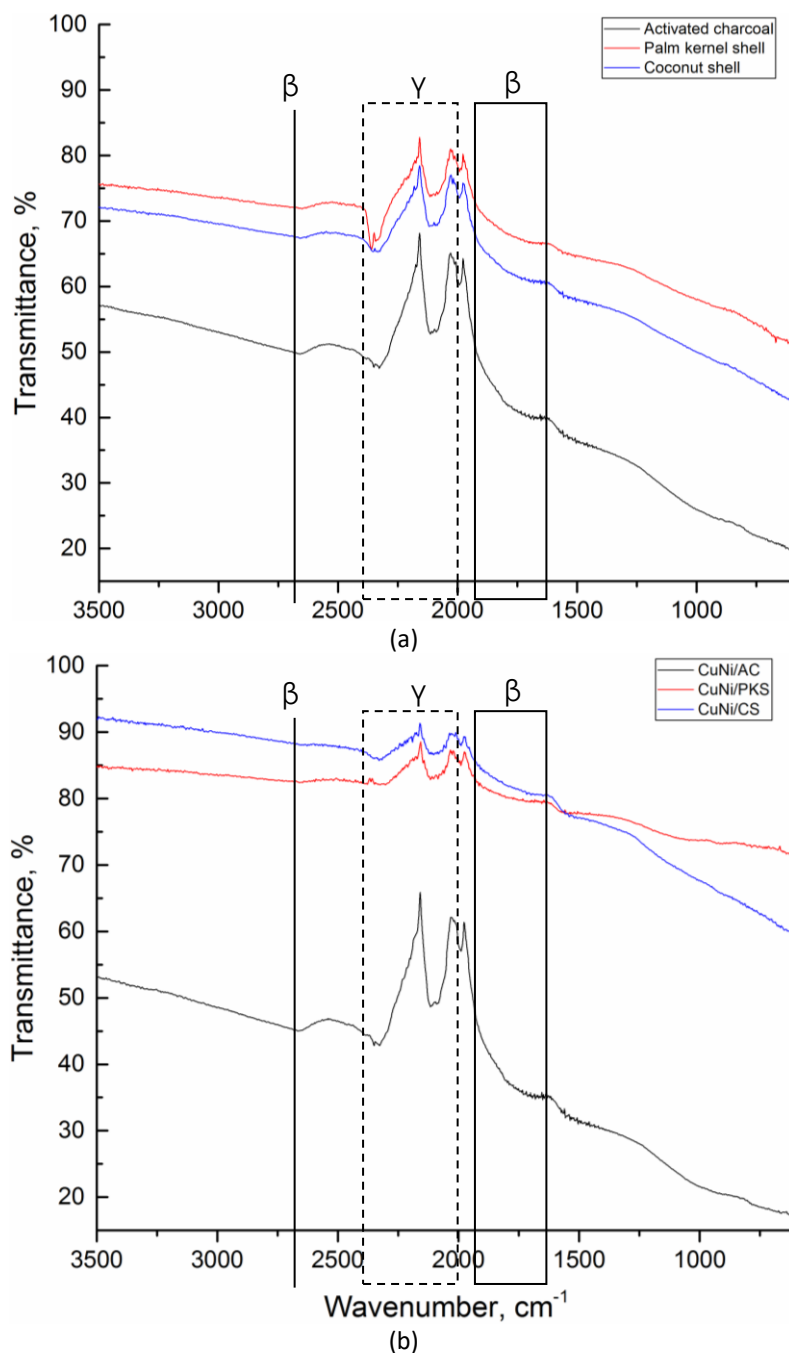


Fig. 3. FTIR spectra for; (a) different carbon supports, and (b) derivative catalysts

3.2 Catalyst Activity

The conversion of glycerol over the carbon catalysts in an inert environment is shown in Figure 4. CuNi/CS has similar glycerol consumption to CuNi/AC, while CuNi/PKS has about 2.5% lower conversion. In this system, the P/dP shows the true equilibrium pressure, so it can be recognized that the glycerol consumption happened in the APR regime as $P/dP > 1.0$ indicates that the water is still in the liquid state. Besides, higher values indicate more gaseous products have been released during the conversion contributing to the total pressure. CuNi/CS was selected to be further investigated because of the competitive consumption with the commercial carbon-supported catalyst (CuNi/AC) and due to the generation of gaseous products. Figure 5 shows the glycerol conversion profile and

formation of a liquid product – acetic acid. It can be observed that acetic acid is gradually formed in the first 200 min and then intensely generated until it stops at the 600th minute with no observable glycerol consumption. The gaseous products were also detected, including carbon monoxide, propylene oxide and acetaldehyde, as determined via deconvolution of the mass spectrum in Figure 6.

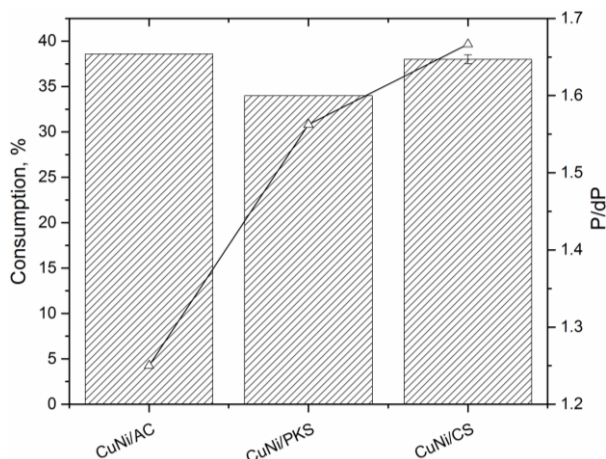


Fig. 4. Effect of catalyst supports on glycerol conversion at 20 wt% initial glycerol concentration, 200 °C, 25 bar and 180 mins

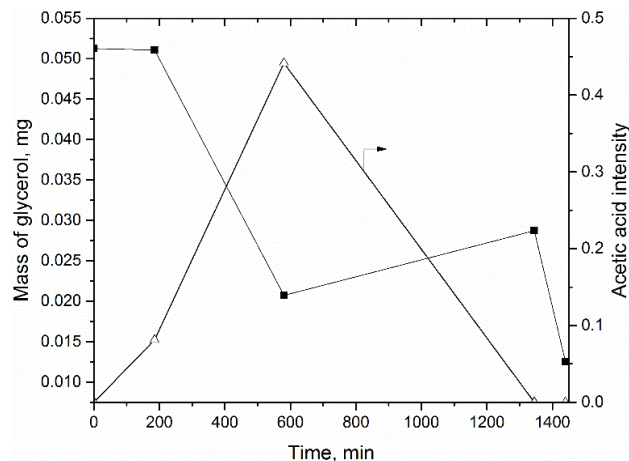


Fig. 5. Glycerol conversion profile over CuNi/CS at 20 wt% initial glycerol concentration, 20 bar and 200 °C

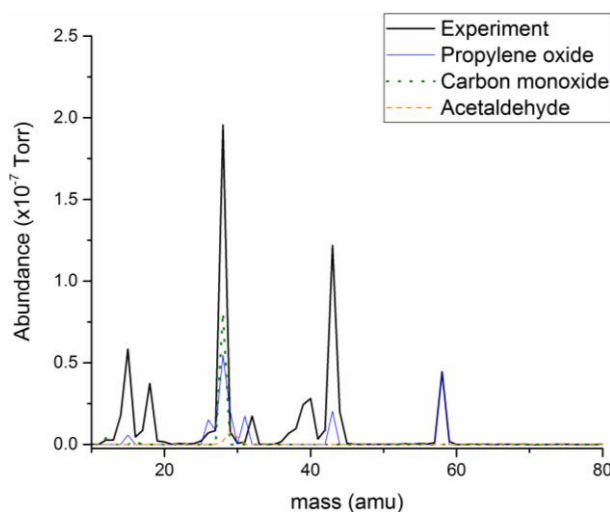


Fig. 6. Deconvolution of MS spectrum of gaseous products

The reaction of glycerol by using CuNi/CS exhibits C-C and C-O bonds breakage and dehydration. Acetic acid is a product of glycerol dehydration to 3-hydroxypropanal, which could produce other compounds such as acetaldehyde, 1,3-propanediol and propanoic acid, if the reaction condition permits [24]. Meanwhile, carbon monoxide is co-generated from glycerol reforming to hydrogen based on Eq. (2). However, no hydrogen detected in the gas-phase products signifying total consumption in the reaction. Glycerol is also suggested to convert to propylene glycol and subsequently dehydrated to propylene oxide [25]. The high C-C and C-O breakages can occur at low temperatures and in an acidic medium [8,23,24]. Therefore, it is proposed that the routes of acetic acid and propylene oxide formation are as illustrated in Figure 7.

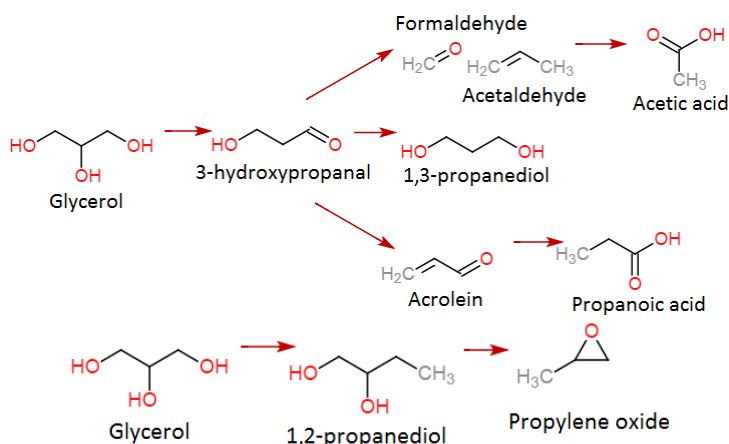


Fig. 7. Proposed mechanism for the aqueous-phase reforming of glycerol over CuNi/CS

Coke may also be formed according to Eq. (3) and Eq. (4), which could deactivate the catalyst. About 10 mg of the catalyst was combusted in a thermogravimetric analyzer TGA4000 (PerkinElmer, UK) at 950 °C to obtain the weight of coke formed. It was observed that the coke formation was constant as the reaction proceeded, suggesting no additional coke that caused the deactivation of the catalyst.



3.3 Effects of Operating Parameters

The influence of operating parameters on glycerol consumption and acetic acid formation was also studied. Figure 8 shows that the glycerol consumption increased from 10 to 38% when increasing the pressure from 20 to 25 bar. The activity of the catalyst was zeroed at higher pressure. The optimum P/P_{sat} was reported in the literature to be 1 to 1.2, while the values for 20, 25 and 30 bar at 200 °C in this study were 1.0, 1.3 and 1.6, respectively [26]. The higher value at 30 bar caused insufficient energy for the reaction to occur at the same temperature. In the meantime, the formation of acetic acid decreased, attributable to the lower formation and degradation of 3-hydroxypropanal. A separate study showed that the selectivity towards 1,3-propanediol formation (also a product of 3-hydroxypropanal reduction) is proportional to the pressure from 1 to 3.6 bar at 190 °C [27]. Furthermore, Rode *et al.*, [28] on using a copper-based catalyst, suggested that the catalyst favors C-O breakage compared to C-C cleavage at high pressure. This means increasing the pressure further does not affect the C-C bond breaking of 3-hydroxypropanal [28].

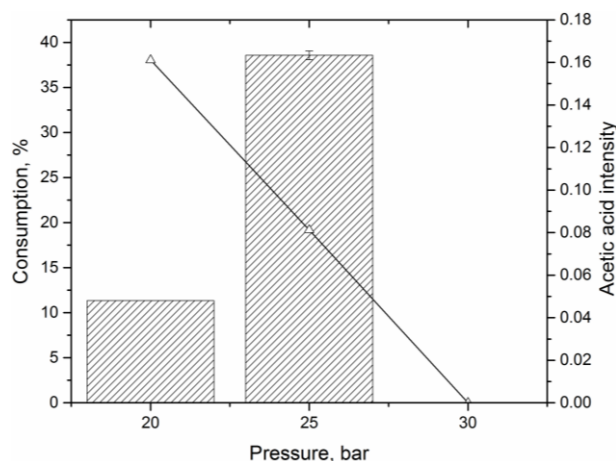


Fig. 8. Effect of operating pressure on glycerol conversion over CuNi/CS at 20 wt% initial glycerol concentration, 200 °C and 180 mins

Figure 9 shows the effect of temperature on glycerol conversion and acetic acid formation. As the temperature increased, the conversion and the production of acetic acid showed a proportionality relationship. However, no acetic acid was formed at a temperature lower than 200 °C. A similar finding was reported by Gandarias *et al.*, [24] where acetic acid production was observed between 220 – 240 °C at 45 bar. It was suggested as a cracked product during glycerol consumption [24]. Nevertheless, it can be implied that the influence of temperature on glycerol consumption is not as pronounced as the influence of pressure.

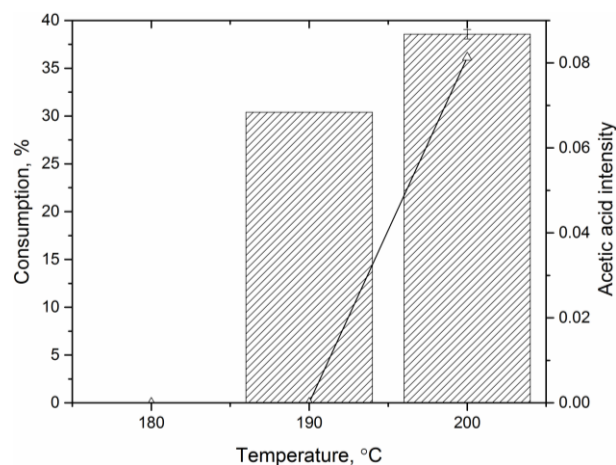


Fig. 9. Effect of operating temperature on glycerol conversion over CuNi/CS at 20 wt% initial glycerol concentration, 25 bar and 180 mins

The experiment of varying the initial glycerol concentration revealed that, in this study, at least 20 wt% is required for consumption. Meanwhile, at higher concentration (30 wt%), no presence of acetic acid in the liquid products was shown (Figure 10). Different products could be formed through a different route of reaction because of the lower saturation pressure at 30 wt% glycerol concentration. This provides another opportunity for research and application of glycerol consumption at higher concentrations.

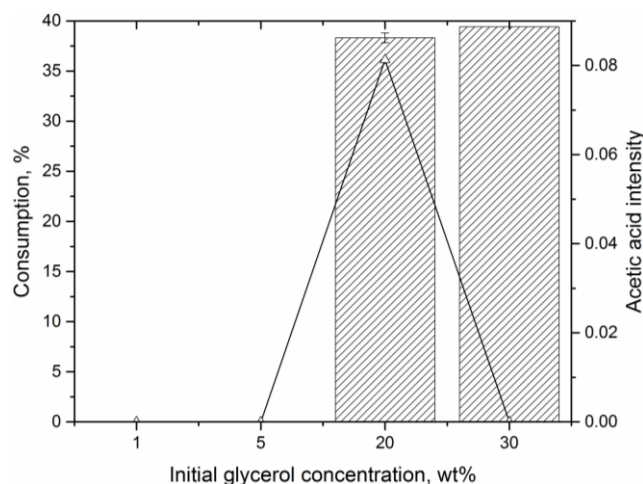


Fig. 10. Effect of initial glycerol concentration on conversion over CuNi/CS at 200 °C, 25 bar and 180 mins

A simulation by Gandarias *et al.*, [24] illustrated that a water-to-glycerol ratio of 9 (about 10 wt%) gave the best glycerol conversion by using a Pt-based catalyst. Considering that this current study uses fewer precious metals as catalysts and could convert glycerol of higher concentration, a promising alternative in glycerol utilization can be provided in the future.

4. Conclusions

Various studies have shown glycerol as a flexible and essential feedstock for producing valuable chemicals via multiple routes involving catalytic conversion. In this study, a CuNi catalyst was impregnated over coconut shell-activated carbon. The BET surface area decreased after the impregnation of the catalyst but the average pore size improved to a smaller value. The catalyst exhibits the presence of carboxylic acids, which is vital in hydrogenolysis or reduction of glycerol into shorter C-C chains. CuNi/CS was used to convert glycerol into value-added products under mild conditions (temperature between 180 to 200 °C and pressure between 20 to 30 bar), also called as aqueous-phase reforming. Among the products detected were acetic acid, carbon monoxide, propylene oxide and acetaldehyde, in which a possible mechanism was proposed. The formation of acetic acid, due to the dehydration of acetaldehyde, decreased with increasing pressure, but was proportional to temperature. It was also found that the acetic acid formation is susceptible to initial glycerol concentration. From a bigger perspective, this work has shown that glycerol utilization under mild conditions and using catalysts developed from agro waste and non-noble catalysts is possible.

Acknowledgement

This research is supported by the Ministry of Higher Education Malaysia under the Fundamental Research Grant Scheme, FRGS/1/2020/WAB02/UNIMAS/03/1. The authors wish to acknowledge the University of Sheffield, UK and Universiti Malaysia Sarawak, Malaysia, for the support of research materials and facilities.

References

- [1] International Energy Agency. "Renewables 2018: Analysis and Forecasts to 2023." *IEA Market Report*, 2018.
- [2] Alimin, Ahmad Jais, and Olawale Kazeem Babalola. "A Review on the Influence of Additive Blended Biodiesel to the Performance and Emission Characteristics of Heavy-Duty Diesel Engines." *Journal of Advanced Research in Fluid Mechanics and Thermal Sciences* 111, no. 1 (2023): 180-193. <https://doi.org/10.37934/arfmts.111.1.180193>

- [3] Mahayuddin, Nurul Eza Maisara Mohd, Sharifah Nur Afiqah Syed Mustaffa, Hafiza Shukor, Jennifer Patero Tamayo, and Farizul Hafiz Kasim. "Biodiesel production in Malaysia: Current status and challenges." In *AIP Conference Proceedings*, vol. 2541, no. 1. AIP Publishing, 2022. <https://doi.org/10.1063/5.0113176>
- [4] Jeswani, Harish K., Andrew Chilvers, and Adisa Azapagic. "Environmental sustainability of biofuels: a review." *Proceedings of the Royal Society A* 476, no. 2243 (2020): 20200351. <https://doi.org/10.1098/rspa.2020.0351>
- [5] Binhayeeding, Narisa, Sappasith Klomklao, and Kanokporn Sangkharak. "Utilization of waste glycerol from biodiesel process as a substrate for mono-, di-, and triacylglycerol production." *Energy Procedia* 138 (2017): 895-900. <https://doi.org/10.1016/j.egypro.2017.10.130>
- [6] Attarbach, Taha, Martin D. Kingsley, and Vincenzo Spallina. "New trends on crude glycerol purification: A review." *Fuel* 340 (2023): 127485. <https://doi.org/10.1016/j.fuel.2023.127485>
- [7] Yuliana, Maria, Luciana Trisna, Feprita Sari, and Valentino Bervia Lunardi. "Glycerol purification using reactivated spent bleaching earth from palm oil refineries: Zero-waste approach." *Journal of Environmental Chemical Engineering* 9, no. 3 (2021): 105239. <https://doi.org/10.1016/j.jece.2021.105239>
- [8] Shoar, Farid Haghghat, Bahman Najafi, Shahab S. Band, Kwok-Wing Chau, and Amir Mosavi. "Different scenarios of glycerin conversion to combustible products and their effects on compression ignition engine as fuel additive: a review." *Engineering Applications of Computational Fluid Mechanics* 15, no. 1 (2021): 1191-1228. <https://doi.org/10.1080/19942060.2021.1961101>
- [9] Berahim, Muhammad Syahizul Aidi, Mohd Fadhil Majnis, and Mustaffa Ali Azhar Taib. "Formation of Titanium Dioxide Nanoparticles by Anodization of Valve Metals." *Progress in Energy and Environment* 7 (2018): 11-19.
- [10] Martin, Andreas, Udo Armbruster, Inaki Gandarias, and Pedro Luis Arias. "Glycerol hydrogenolysis into propanediols using in situ generated hydrogen-A critical review." *European Journal of Lipid Science and Technology* 115, no. 1 (2013): 9-27. <https://doi.org/10.1002/ejlt.201200207>
- [11] Fasolini, Andrea, Daniele Cespi, Tommaso Tabanelli, Raffaele Cucciniello, and Fabrizio Cavani. "Hydrogen from renewables: a case study of glycerol reforming." *Catalysts* 9, no. 9 (2019): 722. <https://doi.org/10.3390/catal9090722>
- [12] Luo, Nianjun, Xun Zhao, Fahai Cao, Tiancun Xiao, and Dingye Fang. "Thermodynamic study on hydrogen generation from different glycerol reforming processes." *Energy & Fuels* 21, no. 6 (2007): 3505-3512. <https://doi.org/10.1021/ef070066g>
- [13] Saeidabad, Nasim Ghaffari, Young Su Noh, Ali Alizadeh Eslami, Hyun Tae Song, Hyun Dong Kim, Ali Fazeli, and Dong Ju Moon. "A review on catalysts development for steam reforming of biodiesel derived glycerol; Promoters and supports." *Catalysts* 10, no. 8 (2020): 910. <https://doi.org/10.3390/catal10080910>
- [14] Roslan, Nurul Asmawati, Sumaiya Zainal Abidin, Asmida Ideris, and Dai-Viet N. Vo. "A review on glycerol reforming processes over Ni-based catalyst for hydrogen and syngas productions." *International Journal of Hydrogen Energy* 45, no. 36 (2020): 18466-18489. <https://doi.org/10.1016/j.ijhydene.2019.08.211>
- [15] Rajeswara, Sarveshini, Muliani Mansor, Nurfatehah Wahyuni Che Jusoh, Azran Mohd Zainoodin, Khairunnisa Mohd Pa'ad, and Shinya Yamanaka. "The Effects of Calcination Temperature of Nickel Supported on Candle Soot towards Ethanol Oxidation Reaction (EOR)." *Journal of Research in Nanoscience and Nanotechnology* 8, no. 1 (2023): 23-30. <https://doi.org/10.37934/jrnn.8.1.2330>
- [16] Azri, Norsahida, Ramli Irmawati, Usman Idris Nda-Umar, Mohd Izham Saiman, and Yun Hin Taufiq-Yap. "Effect of different supports for copper as catalysts on glycerol hydrogenolysis to 1, 2-propanediol." *Journal of King Saud University-Science* 33, no. 4 (2021): 101417. <https://doi.org/10.1016/j.jksus.2021.101417>
- [17] Checa, Manuel, Sergio Nogales-Delgado, Vicente Montes, and José María Encinar. "Recent advances in glycerol catalytic valorization: A review." *Catalysts* 10, no. 11 (2020): 1279. <https://doi.org/10.3390/catal10111279>
- [18] Gallegos-Suarez, Esteban, Antonio Guerrero-Ruiz, Inmaculada Rodríguez-Ramos, and Adolfo Arcoya. "Comparative study of the hydrogenolysis of glycerol over Ru-based catalysts supported on activated carbon, graphite, carbon nanotubes and KL-zeolite." *Chemical Engineering Journal* 262 (2015): 326-333. <https://doi.org/10.1016/j.cej.2014.09.121>
- [19] Yakub, Ibrahim, and James McGregor. "Catalytic Reduction of Nitric Oxide with Hydrogen Using Carbon-Supported d-Metal Catalysts." *Waste and Biomass Valorization* (2022): 1-16.
- [20] Edwin Vasu, A. "Surface modification of activated carbon for enhancement of nickel (II) adsorption." *E-Journal of Chemistry* 5, no. 4 (2008): 814-819. <https://doi.org/10.1155/2008/610503>
- [21] Chin, Tan Yong, Ibrahim Yakub, and Taufiq-Yap Yun Hin. "Evaluation of Catalysts Derived from Palm Kernel Shell Carbon in a Passive NOx Removal from a Diesel Engine Exhaust." *Emission Control Science and Technology* 6 (2020): 336-344. <https://doi.org/10.1007/s40825-020-00164-0>
- [22] Yun, Yang Sik, Claudia E. Berdugo-Díaz, Jing Luo, David G. Barton, Ida Chen, Jieun Lee, and David W. Flaherty. "The importance of Brønsted acid sites on CO bond rupture selectivities during hydrogenation and hydrogenolysis of esters." *Journal of Catalysis* 411 (2022): 212-225. <https://doi.org/10.1016/j.jcat.2022.05.014>

- [23] Yu, Weiqiang, Jie Xu, Hong Ma, Chen Chen, Jing Zhao, Hong Miao, and Qi Song. "A remarkable enhancement of catalytic activity for KBH₄ treating the carbothermal reduced Ni/AC catalyst in glycerol hydrogenolysis." *Catalysis Communications* 11, no. 5 (2010): 493-497. <https://doi.org/10.1016/j.catcom.2009.12.009>
- [24] Gandarias, I., P. L. Arias, J. Requies, M. B. Güemez, and J. L. G. Fierro. "Hydrogenolysis of glycerol to propanediols over a Pt/ASA catalyst: The role of acid and metal sites on product selectivity and the reaction mechanism." *Applied Catalysis B: Environmental* 97, no. 1-2 (2010): 248-256. <https://doi.org/10.1016/j.apcatb.2010.04.008>
- [25] Yu, Zhengxi, Lei Xu, Yingxu Wei, Yingli Wang, Yanli He, Qinghua Xia, Xinzhi Zhang, and Zhongmin Liu. "A new route for the synthesis of propylene oxide from bio-glycerol derivated propylene glycol." *Chemical Communications* 26 (2009): 3934-3936. <https://doi.org/10.1039/b907530e>
- [26] Seretis, A., and P. Tsiakaras. "Hydrogenolysis of glycerol to propylene glycol by in situ produced hydrogen from aqueous phase reforming of glycerol over SiO₂-Al₂O₃ supported nickel catalyst." *Fuel Processing Technology* 142 (2016): 135-146. <https://doi.org/10.1016/j.fuproc.2015.10.013>
- [27] Huang, Long, Yulei Zhu, Hongyan Zheng, Guoqiang Ding, and Yongwang Li. "Direct conversion of glycerol into 1, 3-propanediol over Cu-H₄SiW₁₂O₄₀/SiO₂ in vapor phase." *Catalysis Letters* 131 (2009): 312-320. <https://doi.org/10.1007/s10562-009-9914-1>
- [28] Rode, C. V., A. A. Ghalwadkar, R. B. Mane, A. M. Hengne, S. T. Jadkar, and N. S. Biradar. "Selective hydrogenolysis of glycerol to 1, 2-propanediol: comparison of batch and continuous process operations." *Organic Process Research & Development* 14, no. 6 (2010): 1385-1392. <https://doi.org/10.1021/op1001897>